# A Simple Graphic Method for Analyzing the Polarization State of an Optical System with a Fixed Polarizer and a Rotating Elliptical Retarder

**Nan Wang[1, 2, 3] and Sailing He[1, 2, 4, \*]**

**Abstract**—The trajectory of the polarization state of a monochromatic beam passing through a fixed linear polarizer and a rotating elliptical retarder on the Poincaré sphere is found to be a three-dimensional 8-shaped contour, which is determined as the line of intersection of a right-circular cylinder with the Poincaré sphere. The cylinder is parallel to the $S_3$ axis, and the projection of the contour on the $S_1S_2$ plane is a circle whose center and radius are determined. A method of projecting the three-dimensional geometric relationships to the two-dimensional $S_1S_2$ plane to locate the position of the polarization state of the emerging beam on the Poincaré sphere for a given azimuth of the elliptical retarder is presented, and applied to solve a problem of polarization optics. The proposed graphic method substantially simplifies the polarization state analysis involving elliptical retarders.

## 1. INTRODUCTION

A retarder, which is a polarizing component capable of changing the phase of the optical beam, is widely used in polarization optics [1–3]. The most general case of a retarder is an elliptical retarder, whose eigenpolarizations are orthogonal elliptical polarization states [1]. An elliptical retarder is not only of great theoretical significance, but also occurs frequently in practice. For example, certain crystals [4], combinations of linear retarders [4–6], twisted nematic liquid crystal cells [7], birefringence behavior of an optical fiber [8, 9], transparent birefringent mask [10] can all be treated as elliptical retarders.

Therefore, numerous studies on elliptical retarders have been performed [1–4, 6, 7, 11]. One of the most frequently encountered tasks is to study the commonly used optical system consisting of a linear polarizer and an elliptical retarder. It is always desirable to determine the polarization of the emerging beam when the polarization of the polarizer is fixed and the elliptical retarder is rotated [1–4, 7]. Even though such optical system has been well studied and used to characterize the optical parameters of elliptical retarders [4, 7], the methods adopted by these researches mainly rely on the Jones matrix formalism and the Mueller matrix formalism. However, the matrix algebra concerning elliptical retarders is complex, and the tedious calculations often prevent us from forming a clear and systematic picture how the polarization of the emerging beam evolves as the elliptical retarder is rotated [7]. Therefore, it is alluring for us to develop a graphic method to simplify the problem. Perhaps one of the most straightforward ways to achieve this is to apply the famous conclusion that passage of polarized light through an elliptical retarder corresponds to a rotation on the Poincaré sphere about a certain diameter [5]. However, directly applying the method of rotation in the three-dimensional

space is still inconvenient. Alternatively, the trajectory of the polarization states of a linearly polarized beam passing through a rotating linear retarder has been discussed. The early observations on special cases by Rajagopalan & Ramaseshan [12], Azzam et al. [13], and Sabatke et al. [14] presented that the trajectory is a three-dimensional 8-shaped contour. Later Azzam [15] generalized their results and pointed out that such contour is the line of intersection of a right-circular cylinder with the Poincaré sphere. Recently Salazar & Torres [16] further developed this idea and presented that the trajectory becomes the intersection curve of a cone and the Poincaré sphere when the input polarization is an arbitrary state. The previous studies on the trajectory generated by a rotating linear retarder are instructive, while how to extend the results to the cases of elliptical retarder remains a problem. Another limitation of the previous studies is that they only presented the *trajectory* generated by a rotating retarder. While for practical applications, it is more desirable to point out the specific output polarization state for a given orientation of the retarder. This task, however, is still unresolved [15, 16]

In this paper, we demonstrate that the trajectory of the polarization state of a monochromatic beam passing through a fixed linear polarizer and a rotating elliptical retarder on the Poincaré sphere is still an 8-shaped contour, which is determined as the line of intersection of a right-circular cylinder with the Poincaré sphere. The cylinder is parallel to the $\mathbf{S}_3$ axis, and the projection of the contour on the $\mathbf{S}_1\mathbf{S}_2$ plane is a circle tangent to the equator of the Poincaré sphere. The center and the radius of the circle are determined. Based on these geometric relationships, we further present a method of projection to locate the position of the polarization state of the emerging beam on the Poincaré sphere for a given azimuth of the elliptical retarder. The proposed method converts the three-dimensional geometric relationship to a two-dimensional one, and thus substantially simplifies the problem. Finally, an application of this method is demonstrated to determine the intensity of the beam emerging from an optical system consisting of an elliptical retarder sandwiched by two polarizers.

## 2. THEORY

An elliptical retarder has two eigenpolarization states with different optical path lengths. Fast eigenpolarization refers to the polarization associated with the smaller optical path lengths, while slow eigenpolarization corresponds to the one with larger lengths.We adopt the notation $ER(\theta, \varepsilon, \phi)$ to represent an elliptical retarder introducing a phase shift $\phi > 0$ between its fast eigenpolarization $\mathbf{J}_1$ and its slow eigenpolarization $\mathbf{J}_2$. The polarization ellipse of $\mathbf{J}_1$ has an ellipticity angle $\varepsilon \in [-\pi/4, \pi/4]$ and its major axis $\hat{n}$ is characterized by orientation angle $\theta \in [0, \pi)$ (Fig. 1).
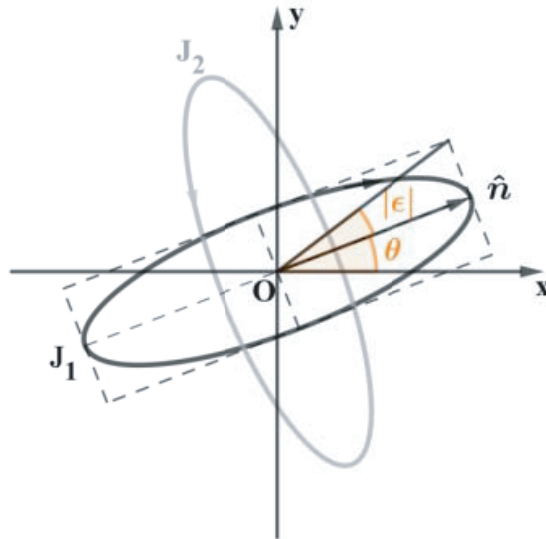


**Figure 1.** Polarization ellipses of eigenpolarization states $\mathbf{J}_1$ and $\mathbf{J}_2$ with major axis $\hat{n}$, orientation angle $\theta$, and ellipticity angle $\varepsilon$ labeled for the ellipse of $\mathbf{J}_1$.

The Jones matrix of elliptical retarder $ER(\theta, \varepsilon, \phi)$ is [7, 11]

$$\mathbf{T} = \begin{bmatrix} \cos(\phi/2) + i\sin(\phi/2)s_1 & \sin(\phi/2)(is_2 + s_3) \\ \sin(\phi/2)(is_2 - s_3) & \cos(\phi/2) - i\sin(\phi/2)s_1 \end{bmatrix}, \tag{1}$$

where

$$\begin{aligned} s_1 &= \cos 2\varepsilon \cos 2\theta \\ s_2 &= \cos 2\varepsilon \sin 2\theta \\ s_3 &= \sin 2\varepsilon. \end{aligned} \tag{2}$$

The Mueller matrix of elliptical retarder $ER(\theta, \varepsilon, \phi)$ can be built from Jones matrix $\mathbf{T}$ by [3]

$$\mathbf{M} = \mathbf{L}\left(\mathbf{T} \otimes \mathbf{T}^*\right)\mathbf{L}^{-1} = \begin{bmatrix} 1 & \mathbf{0} \\ \mathbf{0}^T & \mathbf{m} \end{bmatrix} \tag{3}$$

where $\mathbf{L} = \begin{bmatrix} 1 & 0 & 0 & 1 \\ 1 & 0 & 0 & -1 \\ 0 & 1 & 1 & 0 \\ 0 & i & -i & 0 \end{bmatrix}$, $\otimes$ represents the Kronecker product, asterisk represents complex conjugate, $\mathbf{0} = (0, 0, 0)$, and $\mathbf{m}$ is recognized as the matrix which represents the rotation about axis $\hat{\mathbf{s}} = (\ s_1\ \ s_2\ \ s_3\ )^T$ through angle $-\phi$ on the Poincaré sphere

$$\mathbf{m} = \begin{bmatrix} s_1^2(1 - \cos\phi) + \cos\phi & s_1 s_2(1 - \cos\phi) + s_3\sin\phi & s_1 s_3(1 - \cos\phi) - s_2\sin\phi \\ s_1 s_2(1 - \cos\phi) - s_3\sin\phi & s_2^2(1 - \cos\phi) + \cos\phi & s_2 s_3(1 - \cos\phi) + s_1\sin\phi \\ s_1 s_3(1 - \cos\phi) + s_2\sin\phi & s_2 s_3(1 - \cos\phi) - s_1\sin\phi & s_3^2(1 - \cos\phi) + \cos\phi \end{bmatrix}. \tag{4}$$

Then we consider a beam passing through a fixed linear polarizer with its polarization $\mathbf{P}$ parallel with the $\mathbf{x}$ axis and a rotating elliptical retarder $ER(\theta, \varepsilon, \phi)$ (the angle between the major axis $\hat{n}$ and the $\mathbf{x}$ axis is $\theta$) (Fig. 2). Suppose that the Stokes vector of the beam emerging from the polarizer is $I_0(\ 1\ \ 1\ \ 0\ \ 0\ )^T$, which corresponds to point $A = (\ 1\ \ 0\ \ 0\ )^T$ on the Poincaré sphere. Then the beam emerging from the elliptical retarder $ER(\theta, \varepsilon, \phi)$ has a Stokes vector $I_0\mathbf{M}(\ 1\ \ 1\ \ 0\ \ 0\ )^T$, which corresponds to point $B = \mathbf{m}A$ on the Poincaré sphere. Substituting Equations (2) and (4) into $B = \mathbf{m}A$ gives

$$B = \begin{pmatrix} \cos^2 2\varepsilon \cos^2 2\theta(1 - \cos\phi) + \cos\phi \\ \cos^2 2\varepsilon \cos 2\theta \sin 2\theta(1 - \cos\phi) - \sin 2\varepsilon \sin\phi \\ \cos 2\varepsilon \sin 2\varepsilon \cos 2\theta(1 - \cos\phi) + \cos 2\varepsilon \sin 2\theta \sin\phi \end{pmatrix} = \begin{pmatrix} B_1 \\ B_2 \\ B_3 \end{pmatrix}.$$
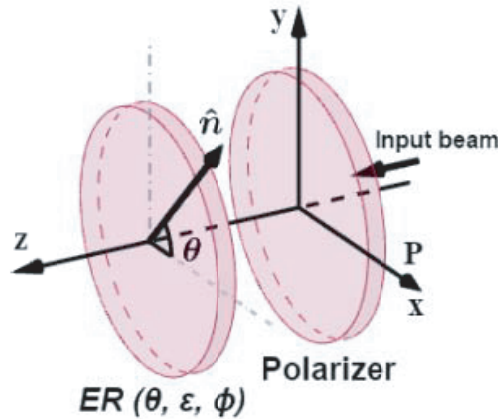


**Figure 2.** The combination of a fixed linear polarizer and a rotating elliptical retarder.

By elimination of $\theta$, we are able to obtain the relationship between $B_1$ and $B_2$: $(B_1 - B_1')^2 + (B_2 - B_2')^2 = r^2$, where

$$B_1' = \cos\phi + 1/2 \ \cos^2 2\varepsilon(1 - \cos\phi)$$
$$B_2' = -\sin 2\varepsilon \sin\phi \tag{5}$$
$$r = 1/2 \cos^2 2\varepsilon(1 - \cos\phi).$$

Therefore, the trajectory of point $B$ (denoted by $b$) on the Poincaré sphere as the elliptical retarder is rotated is the intersection line of the Poincaré sphere and a right-circular cylinder whose axis is parallel with the $\mathbf{S}_3$ axis (Fig. 3(a)). If we denote the projection of trajectory $b$ on the $\mathbf{S}_1\mathbf{S}_2$ plane as $C_B$, then $C_B$ is a circle whose center locates at point $B' = (B_1', B_2', 0)^T$ and radius equals $r$. It can be verified that $\sqrt{B_1'^2 + B_2'^2} + r = 1$. Therefore, circle $C_B$ is tangent to the equator of the Poincaré sphere, and the coordinate of the tangent point $D$ is $D = (B'_1, B'_2, 0)^T/\sqrt{B_1'^2 + B_2'^2}$. In addition, it is worth mentioning that the 8-shaped trajectory generated by rotating elliptical retarder is also understandable from another aspect, if we treat the elliptical retarder as the composition of a linear birefringence and an optical activity and apply the results given by Salazar & Torres [16].
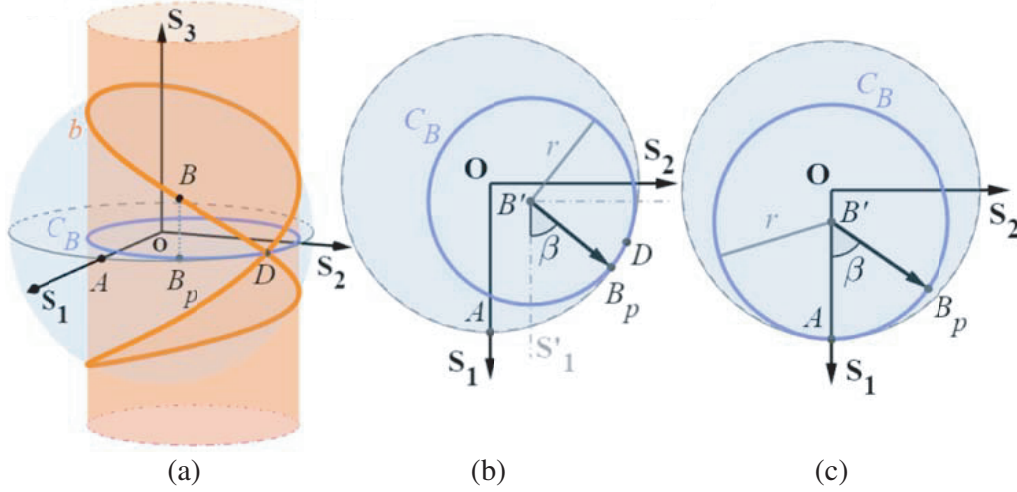


**Figure 3.** (a) When the elliptical retarder is rotated, the trajectory $b$ of point $B$ on the Poincaré sphere is the intersection line of the Poincaré sphere and a right-circular cylinder whose axis is parallel with the $\mathbf{S}_3$ axis. (b) Schematics for locating point $B_p$ associated with a given azimuth $\theta$ of the elliptical retarder on the $\mathbf{S}_1\mathbf{S}_2$ plane. (c) Schematics of projection curve $C_B$ for a linear retarder.

Next, we will show how to locate point $B$ for a given azimuth $\theta$ of the elliptical retarder. When $\theta$ varies, point $B$ moves along curve $b$. This defines a mapping from $[0, \pi)$ to $b$: $\theta \to B(\theta)$. The mapping exhibits a useful property when we observe the $\mathbf{S}_1\mathbf{S}_2$ plane. Suppose that point $B_p$ is the projection of point $B$ on the $\mathbf{S}_1\mathbf{S}_2$ plane, and axis $\overrightarrow{B'S_1'}$ is parallel with the $\mathbf{S}_1$ axis, then angle $\beta$ between $\overrightarrow{B'B_p}$ and $\overrightarrow{B'S_1'}$ satisfies (Fig. 3(b))

$$\beta = 4\theta. \tag{6}$$

This can be verified by $\tan\beta = \frac{B_2 - B_2'}{B_1 - B_1'} = \tan 4\theta$. Equation (6) allows us to locate the position of projection point $B_p$. However, in order to uniquely determine the position of point $B(\theta)$ (except when $B$ coincides with $D$), we still needs to point out whether $B$ locates on the upper or lower hemisphere. This can be achieved by determining the sign of $B_3 = M\sin(2\theta + \gamma)$, where $M = \sqrt{\sin^2\phi + [\sin 2\varepsilon(1 - \cos\phi)]^2} \cos 2\varepsilon \geq 0$, and $\tan\gamma = \sin 2\varepsilon \tan(\phi/2)$ $(\gamma \in [-\pi/2, \pi/2])$. Since $B_3$ and $\sin(2\theta + \gamma)$ have the same sign (when $M \neq 0$), $B(\theta)$ locates on the upper hemisphere if

$\sin(2\theta + \gamma) > 0$ and on the lower hemisphere if $\sin(2\theta + \gamma) < 0$. In summary, our graphic method to determine the output polarization state associated with a given azimuth $\theta$ of the elliptical retarder has two steps: (i) construct circle $C_B$ by Equation (5), (ii) point out the position of $B$ by equation (6) and the sign of $\sin(2\theta + \gamma)$. Above procedures can be accomplished by a simple sketch on the $\mathbf{S}_1\mathbf{S}_2$ plane (Fig. 3(b)), do not involve complicated calculations, and thus substantially simplify the determination of the output polarization state.

In addition, when $\sin(2\theta + \gamma) = 0$, $B$ coincides with $D$, which means that the elliptical retarder converts a linear polarized beam into another linear polarized beam. When $M \neq 0$, there are only two values of $\theta$ which will achieve this. For $M = 0$ (such as a linear $\lambda/2$ retarder and circular retarders), the elliptical retarder converts any linear polarized beam into a linear polarized beam regardless the value of $\theta$.

Furthermore, it should be noted that our graphic method also simplifies the problems concerning a linear retarder, which is only a special case of elliptical retarders. For a linear retarder, $\varepsilon = 0$, $B_2' = 0$, and thus the center of $C_B$ is on the $\mathbf{S}_1$ axis (Fig. 3(c)). This is the result given by Azzam [15] and Salazar & Torres [16], however, we can further determine the position of $B$ associated with $\theta$. Still $B_p$ can be obtained by Equation (6), and the hemisphere $B(\theta)$ locates is determined by $\theta$: it locates on the upper hemisphere when $\theta \in (0, \pi/2)$ and on the lower hemisphere when $\theta \in (\pi/2, \pi)$, since $\gamma = 0$.

## 3. APPLICATION

As a demonstration to show the convenience of our graphic method, we apply it to an optical system which besides the configuration shown in Fig. 2 has another rotating linear polarizer (called analyzer) after the elliptical retarder (Fig. 4). Suppose the angle between polarization $\mathbf{A}$ of the analyzer and the $\mathbf{x}$ axis is $\alpha$, then we will determine the intensity of the beam emerging from the whole system for arbitrary values of $\alpha$ and $\theta$.
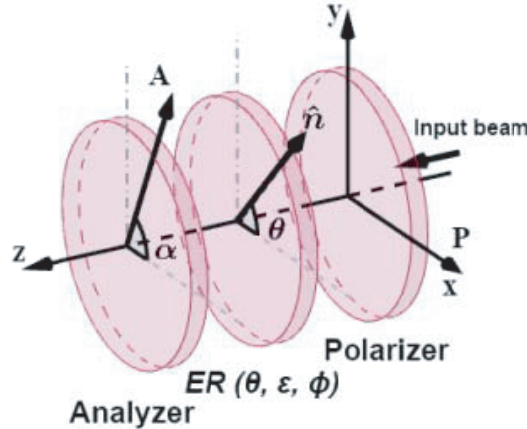


**Figure 4.** The combination of a fixed polarizer, a rotating elliptical retarder, and a rotating analyzer.

In order to do this, we adopt the graphic representation of a polarizer on the Poincaré sphere (Fig. 5(a)). When an elliptically polarized beam with Stokes vector $I_0(\ 1\quad B_1\quad B_2\quad B_3\ )^T$ passes through an analyzer rotated about the z axis through angle $\alpha$, the intensity of the output beam is $I = (1 + \cos)I_0/2$, where $R = (\ \cos 2\alpha\quad \sin 2\alpha\quad 0\ )^T$ representing a point on the equator of the Poincaré sphere, $B = (\ B_1\quad B_2\quad B_3\ )^T$, and is the arc of the great circle [2]. By applying spherical law of cosines in the spherical triangle $BNR$ ($N$ is the north pole of the Poincaré sphere), we have $\cos = \cos\varepsilon_B \cos(2\alpha - \theta_B) = k$, where $\theta_B$ and $\varepsilon_B$ are orientation angle and ellipticity angle of the polarization ellipse represented by point $B$, $k$ satisfying $\overrightarrow{OB_R} = k\overrightarrow{OR}$ is the "ratio" of $\overrightarrow{OB_R}$ and $\overrightarrow{OR}$, and $B_R$ is the projection of $B$ on the $\overrightarrow{OR}$ axis. Therefore, the intensity can be finally simplified as $I = (1 + k)I_0/2$.
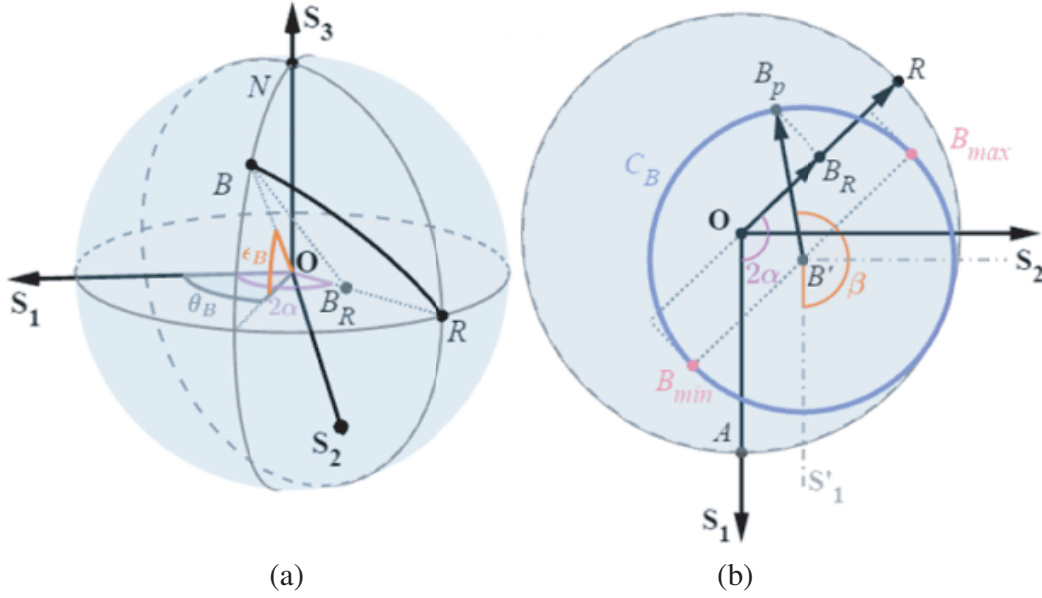
**Figure 5.** (a) The intensity of the emerging beam from a linear polarizer is $I = (1 + \cos)I_0/2($ is the arc of the great circle), when the polarization state of the incident beam with intensity $I_0$ is represented by point $B$ on the surface of the Poincaré sphere and point $R = (\ \cos 2\alpha \quad \sin 2\alpha \quad 0\ )^T$ is determined by the azimuth $\alpha$ of the polarizer. (b) Schematics for obtaining the intensity of a beam passing through a polarizer, an elliptical retarder and an analyzer by geometric relationships on the $\mathbf{S}_1\mathbf{S}_2$ plane.

Like what we did before, we can then obtain the output intensity simply by working on the $\mathbf{S}_1\mathbf{S}_2$ plane (Fig. 5(b)). More specifically, first construct circle $C_B$, then point out $B_p$ by Equation (6), next construct point $R = (\ \cos 2\alpha \quad \sin 2\alpha \quad 0\ )^T$, after that project $B_p$ on the $\overrightarrow{OR}$ axis to obtain $B_R$ and $k$, and finally the intensity of the output beam is $I = (1 + k)I_0/2$.

Compared with matrix calculations, this method provides us with deeper insight and can visually demonstrate how the output intensity varies with $\alpha$ and $\theta$. Such advantage is even further enlarged during getting analytical solutions concerning the extreme values of the output intensities. For example, when the analyzer is fixed ($\alpha$ remains constant) and the elliptical retarder is rotated, we can instantly identify from Fig. 5(b) that the intensity of the output beam takes its maximum $I_{\max}$ when $\beta = 4\theta = 2\alpha$ or $\beta = 4\theta = 2\alpha + 2\pi$ ($B_p$ coincides with point $B_{\max}$) and takes its minimum $I_{\min}$ when $\beta = 4\theta = 2\alpha + \pi$ or $\beta = 4\theta = 2\alpha + \pi \pm 2\pi$ ($B_p$ coincides with point $B_{\min}$). This result allows us to experimentally determine (not uniquely) the orientation of major axis $\hat{n}$. Furthermore, the general form of $I_{\max}$ and $I_{\min}$ can be obtained by geometric relationship without difficulty, however, as a demonstration we only present the results when $\alpha = 0$ and $\alpha = \pi/2$, since these are the most frequently encountered situations (where $I_{\max}$ and $I_{\min}$ take simpler forms). When $\alpha = 0$, we have

$$I_{\max}^{\alpha=0} = I|_{\theta=0 \ or \ \frac{\pi}{2}}^{\alpha=0} = \frac{1}{2}\left(1 + B_1|_{\theta=0 \ or \ \frac{\pi}{2}}\right)I_0$$

$$= \frac{1}{2}\left(1 + \cos\phi + \cos^2 2\varepsilon\,(1 - \cos\phi)\right)I_0 \tag{7}$$

$$I_{\min}^{\alpha=0} = I|_{\theta=\frac{\pi}{4} \ or \ \frac{3\pi}{4}}^{\alpha=0} = \frac{1}{2}\left(1 + B_1|_{\theta=\frac{\pi}{4} \ or \ \frac{3\pi}{4}}\right)I_0 = \frac{1}{2}\left(1 + \cos\phi\right)I_0.$$

When $\alpha = \pi/2$, we have

$$I_{\max}^{\alpha=\pi/2} = I|_{\theta=\frac{\pi}{4} \ or \ \frac{3\pi}{4}}^{\alpha=\pi/2} = \frac{1}{2}\left(1 - B_1|_{\theta=\frac{\pi}{4} \ or \ \frac{3\pi}{4}}\right)I_0 = \frac{1}{2}\left(1 - \cos\phi\right)I_0$$

$$I_{\min}^{\alpha=\pi/2} = I|_{\theta=0 \ or \ \frac{\pi}{2}}^{\alpha=\pi/2} = \frac{1}{2}\left(1 - B_1|_{\theta=0 \ or \ \frac{\pi}{2}}\right)I_0 = \frac{1}{4}\left(1 - \cos\phi\right)\left(1 - \cos 4\varepsilon\right)I_0. \tag{8}$$

Combining Equations (7) and (8), we can relate the parameters of the elliptical retarder to the intensity of the emerging beam by

$$
\cos 4\varepsilon = 1 - \frac{2I_{\min}^{\alpha=\pi/2}}{I_{\max}^{\alpha=\pi/2}}
$$

$$
\cos \phi = \frac{I_{\min}^{\alpha=0} - I_{\max}^{\alpha=\pi/2}}{I_{\max}^{\alpha=\pi/2} + I_{\min}^{\alpha=0}}.
$$

(9)

In contrast, obtaining the analytical solutions of Equations (7)–(9) by matrix calculations requires complex matrix multiplications and computing the derivative of the output intensity, which are apparently not as convenient and clear as our graphic method.

## 4. CONCLUSION

In this paper, a detailed analysis of the fixed-polarizer rotating-elliptical-retarder optical system by a graphic method has been presented. The trajectory of the polarization state of the beam emerging from the system is an 8-shaped contour, which is determined as the intersection line of the Poincaré sphere and a right-circular cylinder whose axis is parallel with the $\mathbf{S}_3$ axis. The projection of the trajectory on the $\mathbf{S}_1\mathbf{S}_2$ plane is a circle whose center and radius are determined. Furthermore, the polarization state of the emerging beam associated with a given azimuth of the elliptical retarder can be easily obtained. This method converts the complicated problem of polarization optics to a simple two-dimensional geometric issue, and its convenience and effectiveness have been demonstrated by determining the intensity of the beam emerging from an optical system consisting of an elliptical retarder sandwiched by two polarizers.

## REFERENCES

1. Chipman, R. A., W.-S. T. Lam, and G. Young, *Polarized Light and Optical Systems*, CRC Press, 2018.
2. Goldstein, D. H., *Polarized Light*, CRC Press, 2017.
3. Gil, J. J. and R. Ossikovski, *Polarized Light and the Mueller Matrix Approach*, CRC Press, 2017.
4. El-Hosseiny, F., "Methods for determining the optical parameters of elliptic retarders," *J. Opt. Soc. Am.*, Vol. 65, 1279–1282, 1975.
5. Pancharatnam, S., "Achromatic combinations of birefringent plates," *Proceedings of the Indian Academy of Sciences — Section A*, 137–144, Springer, 1955.
6. Gottlieb, D. and O. Arteaga, "Optimal elliptical retarder in rotating compensator imaging polarimetry," *Opt. Lett.*, Vol. 46, 3139–3142, 2021.
7. Lin, P.-L., C.-Y. Han, and Y.-F. Chao, "Three-intensity measurement technique and its measurement in elliptical retarder," *Opt. Commun.*, Vol. 281, 3403–3406, 2008.
8. Eugui, P., D. J. Harper, A. Lichtenegger, M. Augustin, C. W. Merkle, A. Woehrer, C. K. Hitzenberger, and B. Baumann, "Polarization-sensitive imaging with simultaneous bright-and dark-field optical coherence tomography," *Opt. Lett.*, Vol. 44, 4040–4043, 2019.
9. Chung, D., H. S. Park, F. Rotermund, and B. Y. Kim, "Measurement of bending-induced birefringence in a hollow-core photonic crystal fiber," *Opt. Lett.*, Vol. 44, 5872–5875, 2019.
10. Vella, A. and M. A. Alonso, "Poincaré sphere representation for spatially varying birefringence," *Opt. Lett.*, Vol. 43, 379–382, 2018.

11. Yu, C.-J., "Fully variable elliptical phase retarder composed of two linear phase retarders," *Rev. Sci. Instrum.*, Vol. 87, 035106, 2016.

12. Rajagopalan, S. and S. Ramaseshan, "Rotating elliptic analysers for the automatic analysis of polarised light — Part I," *Proceedings of the Indian Academy of Sciences — Section A*, 297–312, Springer, 1964.

13. Azzam, R., T. Bundy, and N. Bashara, "The fixed-polarizer nulling scheme in generalized ellipsometry," *Opt. Commun.*, Vol. 7, 110–115, 1973.

14. Sabatke, D., M. Descour, E. Dereniak, W. Sweatt, S. Kemme, and G. Phipps, "Optimization of retardance for a complete Stokes polarimeter," *Opt. Lett.*, Vol. 25, 802–804, 2000.

15. Azzam, R., "Poincaré sphere representation of the fixed-polarizer rotating-retarder optical system," *J. Opt. Soc. Am. A*, Vol. 17, 2105–2107, 2000.

16. Salazar-Ariza, K. and R. Torres, "Trajectories on the Poincaré sphere of polarization states of a beam passing through a rotating linear retarder," *J. Opt. Soc. Am. A*, Vol. 35, 65–72, 2018.